

# Effect of Infrared Drying Power on Dehydration Characteristics, Energy Consumption, and Quality Attributes of Common Wormwood (*Artemisia absinthium* L.) Leaves

M. Beigi<sup>1</sup>

## ABSTRACT

In the present work, the effect of infrared drying power on dehydration and rehydration characteristics, energy consumption, and essential oil yield of common wormwood leaves was studied. Thin layers of the leaves were dried at power levels of 200, 300, 400, and 500W. Effective moisture diffusivity values for the leaves over the applied drying conditions were obtained to be in the range of  $8.84 \times 10^{-8}$ - $2.76 \times 10^{-7}$  m<sup>2</sup> s<sup>-1</sup>. Rehydration curves for the dried leaves were obtained at constant temperature of 80°C and fitted to Peleg model. Rehydration capacity of the leaves decreased with increasing infrared drying power. In comparison with the fresh levels, infrared drying caused both increment and decrement in essential oil yield. The highest and the lowest oil yields were obtained from the samples dried at the power levels of 200 and 500W, respectively. Specific energy consumption changed from 4.22 to 10.56 MJ kg<sup>-1</sup>.

**Keywords:** Essential oil, Moisture diffusivity, Rehydration capacity, Specific energy consumption.

## INTRODUCTION

Quality of agricultural products during postharvest period is affected by the moisture content. Generally, high moisture contents of the fresh products prevent safe storage since the existing water participates in microbial and chemical interplays leading to quality deterioration (Torki-Harchegani *et al.*, 2016b). Drying, water removal by application of heat, is the most common technique applied by humans to preserve foods. Reducing water content minimizes the chemical, physical, and nutrient changes, and leads to safe preservation, easy handling, and diversity of usage (Šumic *et al.*, 2016).

Generally, due to inherent properties of fresh materials as well as expected qualities for dried products, fruits and vegetables are

dried as thin layers. In thin-layer drying, mathematical modeling and determination of mass transfer characteristics are possible which are useful to simulate drying curves of materials, design new or improve the existing dryers as well as for the control of the drying process (Onwude *et al.*, 2016). In the literature, numerous studies have been reported on mathematical modeling of dehydration curves and determination of moisture diffusivity for various biological products under different drying methods such as infrared drying of saffron stigmas (Akhondi *et al.*, 2011), vacuum and microwave drying of pomegranate arils (Minaei *et al.*, 2012), and infrared drying of button mushroom slices (Doymaz, 2014).

In spite of possible advantages for the industrial dryers, use of these methods have some key challenges which should be taken into consideration. Ensuring high energy

<sup>1</sup> Department of Mechanical Engineering, Tiran Branch, Islamic Azad University, Tiran, Islamic Republic of Iran.

\* Corresponding author; e-mail: mohsenbeigi59@gmail.com



consumption efficiency is the most important problem in drying technology where large amounts of energy are consumed and release carbon oxides to the environment. Drying process not only consumes great amount of energy, but also could cause some undesirable changes in physical and chemical properties of biological products (Toriki-Harchegani *et al.*, 2012). Hence, it is necessary to use proper technologies and methods to reduce energy consumption during drying process as well as prevent undesirable changes (Beigi, 2016). Among different types of industrial dryers, infrared energy is one of the effective methods that can be used for drying of moist products with some distinct advantages such as shorter drying time, high quality of food products, and high energy efficiency (Doymaz, 2014).

The common wormwood (*Artemisia absinthium* L.) has fibrous roots and straight grooved, branched and silvery-green stems. This herbaceous-perennial plant grows to 120 cm tall. Its leaves are arranged spirally, covered with silky silvery-white trichomes, and bear minute oil-producing glands. The basal leaves are up to 25 cm long, less divided and with short petioles. The health benefits of wormwood essential oil can be attributed to its properties as an anti-helmitic, cholagogue, deodorant, digestive, emenagogue, febrifuge, insecticide, narcotic, vermifuge, and tonic substance. Wormwood is also known as green ginger and absinthium.

The main objectives of the present study were to dry fresh common wormwood leaves using infrared energy at different power levels to (1) investigate dehydration behavior of the leaves, (2) fit the experimental data to some thin layer models, (3) calculate the effective diffusivity, (4) consider and modelling of rehydration curves of the dried leaves, (5) determine extracted essential oil yield from the leaves, and (6) determine specific energy consumption of drying process.

## MATERIALS AND METHODS

### Experiments

The aerial parts of common wormwood (to a height of 5 cm above the ground) were harvested manually before flowering from Chaharmahal-va-Bakhtiari Province farms, central Iranian plateau in May/June 2016. The leaves were separated accurately and stored in a refrigerator at 4–6°C until use. To determine the initial moisture content of the leaves, four samples (50 g) of the fresh material were placed in an oven at 105 °C for 24 h and the average value was determined to be  $2.67 \pm 0.021$  g<sub>water</sub> g<sup>-1</sup><sub>dry matter</sub>.

To conduct the drying experiments, a convective infrared oven was designed and fabricated. Prior to the experiments, the samples were taken out from the refrigerator and placed at room temperature for 2 hours to reach thermal equilibrium with the environment. In each experiment, the leaves (200 g with a thickness of 3 cm) were placed on the drying chamber. The drying experiments were performed at IR powers of 200, 300, 400, and 500W. During the drying process, the sample lot was weighed accurately to 0.01 g (Shimadzu, model UW6200H, Japan) at regular time intervals of 2 minutes and the instantaneous moisture content was determined.

### Mathematical Modeling of Drying Kinetics

The obtained values for moisture content of the leaves during the drying experiments were expressed as Moisture Ratio (MR) using the following equation:

$$MR = \frac{M_i - M_e}{M_0 - M_e} \quad (1)$$

Where,  $MR$  is the dimensionless moisture content ratio; and  $M_i$ ,  $M_0$  and  $M_e$  are the instantaneous moisture content at any given time (g<sub>water</sub> g<sup>-1</sup><sub>dry matter</sub>), the initial moisture

content, and the equilibrium moisture content, respectively.

The  $MR$  data were fitted to the selected thin layer models using nonlinear regression technique and curve fitting tool of MATLAB 7.10 (MathWorks, Inc., Natick, MA). The Root Mean Square Error (RMSE) and coefficient of determination ( $R^2$ ) were used to evaluate and compare the fit goodness of the applied models.

### Determination of Effective Moisture Diffusivity (D)

Moisture removal from biological materials such as fruits and vegetables during drying is mainly controlled by diffusion phenomenon. Fick's second law of transient diffusion can be used to illustrate the moisture transfer in the falling rate period in the following form:

$$\frac{\partial M}{\partial t} = D\nabla^2 M \quad (2)$$

Supposing uniform initial moisture distribution, negligible external resistance and shrinkage, and constant temperature and moisture diffusivity through the drying process, Crank (1975) solved Equation (2) for different solid geometries. For an infinite slab the Crank solution is written as (Crank, 1975):

$$MR = \frac{8}{\pi^2} \sum_{n=1}^{\infty} \frac{1}{(2n-1)^2} \exp\left(-\frac{(2n-1)^2 \pi^2 Dt}{2L^2}\right) \quad (3)$$

Where,  $D$ ,  $L$ , and  $t$  are the effective diffusivity ( $\text{m}^2 \text{s}^{-1}$ ), half thickness of slab (m), and the drying time (s), respectively.

For long drying periods, only the first term of the series is significant, then, the solution becomes:

$$MR = \frac{8}{\pi^2} \exp\left(-\frac{\pi^2 Dt}{2L^2}\right) \quad (4)$$

Equation (4) can be written in logarithmic form:

$$\ln(MR) = \ln\left(\frac{8}{\pi^2}\right) - \left(\frac{\pi^2 Dt}{2L^2}\right) \quad (5)$$

Plotting the graph of  $\ln(MR)$  versus drying time (s), and using slope of the obtained line, the effective diffusion is determined as:

$$D = \left(-\frac{2L^2}{\pi^2}\right) \times \text{Slope} \quad (6)$$

### Rehydration

Rehydration characteristics of the wormwood leaves were determined by immersing the dried leaves in distilled water maintained at  $80^\circ\text{C}$ . Five g of the dried leaves was weighed accurately and placed into a 250 mL beaker containing 150 mL distilled water, agitated and allowed to rehydrate for 5 hours. The samples were removed from the water at every 20 min intervals, drained and weighed with a digital balance accurate to 0.01.

To simulate the water absorption by the dried leaves, the Peleg was used. Peleg equation can be written as follows:

$$\frac{t}{M_i - M_0} = k_1 + k_2 t \quad (7)$$

$$M_e = M_0 + \frac{1}{k_2} \quad (8)$$

Where,  $k_1$  is the Peleg rate constant [ $(\text{g water g}^{-1} \text{ dry matter)}^{-1}$ ] and  $k_2$  is the Peleg capacity constant [ $(\text{g water g}^{-1} \text{ dry matter)}^{-1}$ ].

The equilibrium moisture content of the rehydrated leaves was determined by continuing rehydration process until no water absorption by the leaves. By using the obtained equilibrium moisture content of the rehydrated leaves,  $k_2$  was determined by applying Equation (8) and, then, Equation (7) was used to fit the experimental rehydration data and  $k_1$  was obtained.

### Extraction of Essential Oil

About 100 g of the fresh and 40 g of the dried leaves were used for essential oil extraction. The leaves were isolated by hydro-distillation using a Clevenger-type apparatus. The samples were added to a 2,000 mL flask containing 1,000 mL distilled water and heated for 4 hours. The collected essential oil content was determined and expressed in  $\text{g } 100 \text{ g}^{-1} \text{ dry matter}$ .



## Specific Energy Consumption

Specific Energy Consumption (SEC) for the drying process was calculated using the following equation:

$$SEC = \frac{E}{m_w} \quad (9)$$

Where,  $E$  is the consumed energy (MJ) and  $m_w$  is the mass of removed water (kg) from the samples during drying process.

## RESULTS AND DISCUSSION

### Drying Kinetics

Figure 1 presents the typical drying curves for the common wormwood leaves at the different infrared powers. As expected, drying duration was decreased as infrared radiation power increased where the average process duration at IR powers of 200, 300, 400, and 500W was found to be 56, 44, 36, and 24 minutes, respectively. Generally, higher IR power level leads to higher temperature resulting in increased vapor pressure in the samples and causes faster moisture removal from inside to surface of the product. Also, higher temperatures enhance heat transfer between thermal source and drying material which accelerate

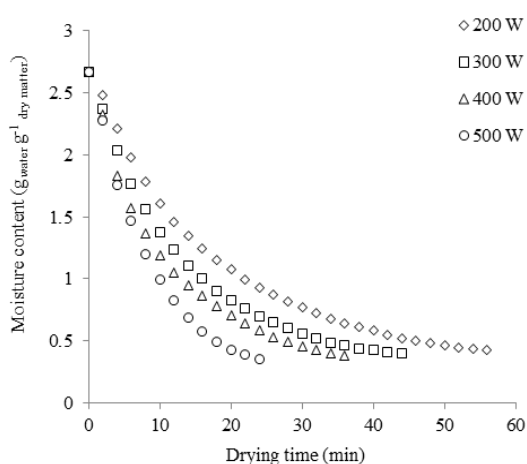


**Figure 1.** Variation in moisture content of the wormwood leaves with drying time at different IR power levels.

moisture evaporation from the material surface and reduce drying time. Similar observations have been reported in terms of influence of infrared power on the drying time of different products such as onion (Sharma *et al.*, 2005), carrot (Doymaz, 2015), and pomegranate seeds (Doymaz, 2012).

Variations of drying rate ( $\text{g water g}^{-1} \text{ dry matter min}^{-1}$ ) of the common wormwood leaves during infrared drying for the different applied powers are shown in Figure 2. The results indicate that drying rates increased rapidly during an initial stage of drying (warming-up period) followed by a falling rate period when drying rate continuously decreased along with decreasing moisture content. Since the radiation absorptivity of foods increases with an increase in moisture content, thermal energy obtained from IR was more absorbed by the leaves during the initial stage of the process, when the samples moisture content was still high. With the product drying out subsequently, heat penetration through the dried layer decreased, thus retarding the drying rates. The same observations have been reported in the literature for IR drying of different biological products by Celma *et al.* (2009) and Akhondi *et al.* (2011). However, some researchers investigated the use of IR-convective drying for some products such as

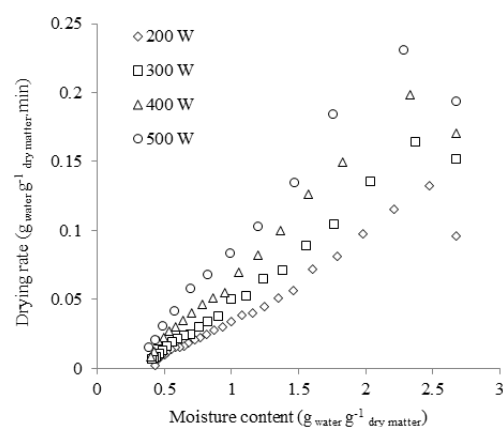


**Figure 2.** Variation in drying rate of the wormwood leaves with moisture content at different IR power levels.

onion (Sharma *et al.*, 2005) and berries (Puente-Díaz *et al.*, 2013), and stated that the warming-up period was not observed. This is probably because forced convection in the drying chamber accelerated the cooling effect, which reduced the temperature of the IR radiator and of the sample. After the warming-up period, the drying process took place in the falling rate period, as indicated by a steady decrease in the drying rate.

### Fitting of Drying Curves

Table 1 presents the obtained statistical analyses results fitting of the drying curves. From the table, it can be concluded that, among the applied models, diffusion approach model was the best to describe the drying curves at all IR power levels used in the experiments. Furthermore, to assess the validity of the diffusion approach model, the experimental moisture ratio values were

**Table 1.** Values of drying constants and coefficients of the mathematical models with statistical analysis for the wormwood leaves.

Model	IR power (W)	Constants and coefficients	RMSE	R <sup>2</sup>
Newton $MR = \exp(-kt)$	200	$k = 0.04179$	0.03764	0.9758
	300	$k = 0.05662$	0.03845	0.9760
	400	$k = 0.06957$	0.04433	0.9686
	500	$k = 0.09582$	0.01794	0.9961
Page $MR = \exp(-kt^n)$	200	$k = 0.07535, n = 0.8179$	0.01822	0.9945
	300	$k = 0.09885, n = 0.8118$	0.01787	0.9951
	400	$k = 0.12651, n = 0.7836$	0.01961	0.9942
	500	$k = 0.1071, n = 0.9539$	0.01683	0.9968
Henderson and Pabis $MR = a \exp(-kt)$	200	$a = 0.9445, k = 0.03904$	0.03323	0.9818
	300	$a = 0.9431, k = 0.05287$	0.03403	0.9821
	400	$a = 0.9352, k = 0.06429$	0.03932	0.9767
	500	$a = 0.9971, k = 0.09551$	0.01872	0.9960
Logarithmic $MR = a \exp(-kt) + b$	200	$a = 0.8729, b = 0.1333, k = 0.05933$	0.00754	0.9991
	300	$a = 0.8775, b = 0.1241, k = 0.07881$	0.00508	0.9996
	400	$a = 0.8654, b = 0.1314, k = 0.09911$	0.01529	0.9967
	500	$a = 0.9543, b = 0.0608, k = 0.1119$	0.01211	0.9985
Midilli $MR = a \exp(-kt^n) + bt$	200	$a = 1.016, b = 0.00159, k = 0.0631, n = 0.9285$	0.00829	0.9990
	300	$a = 1.008, b = 0.00203, k = 0.0805, n = 0.9259$	0.00596	0.9995
	400	$a = 1.013, b = 0.00202, k = 0.1127, n = 0.8743$	0.01475	0.9971
	500	$a = 1.006, b = 0.00287, k = 0.0945, n = 1.059$	0.01211	0.9985
Diffusion Approach $MR = a \exp(-kt) + (1-a) \exp(-kbt)$	200	$a = 0.7504, b = 0.1576, k = 0.06636$	0.006974	0.9992
	300	$a = 0.7991, b = 0.1208, k = 0.08548$	0.00439	0.9997
	400	$a = 0.5608, b = 0.2243, k = 0.1445$	0.01157	0.9981
	500	$a = 0.9987, b = 0.1457, k = 0.0998$	0.01091	0.9985



compared with the predicted ones and the results are presented in Figure 3. As shown, the predicted moisture ratios are in good agreement with the experimental data where the points are generally placed on the 45° straight line. Suitability of the diffusion approach model for describing drying curves has been reported by Zomorodian and Moradi (2010) for *Cuminum cyminum* and Sacilik *et al.* (2006) for organic tomato.

### Effective Moisture Diffusivity (D)

Effective moisture diffusivity values for the wormwood leaves were calculated by using Equation (6) and obtained to be  $8.84 \times 10^{-8}$ ,  $1.58 \times 10^{-7}$ ,  $1.97 \times 10^{-7}$  and  $2.76 \times 10^{-7} \text{ m}^2 \text{ s}^{-1}$  for IR powers of 200, 300, 400 and 500W, respectively. The results declare that any increment in IR power increased moisture diffusivity. In fact, increment in the power level causes a rapid rise in sample temperature leading to higher vapor pressure and faster drying. The diffusivities obtained in this study are comparable with the reported values in the literature for infrared drying of different agricultural and food products such as button mushrooms ( $3.81 \times 10^{-10}$ – $4.20 \times 10^{-9} \text{ m}^2 \text{ s}^{-1}$ ) (Doymaz, 2014) and carrot ( $2.45 \times 10^{-9}$  to  $7.38 \times 10^{-9} \text{ m}^2 \text{ s}^{-1}$ ) (Doymaz, 2015).

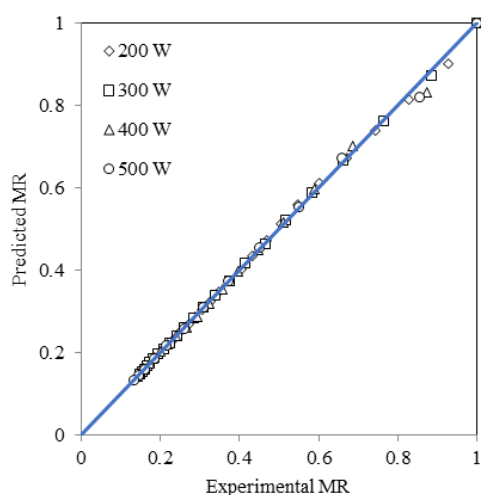


**Figure 3.** Comparison of experimental moisture ratio values with values predicted by diffusion approach model at different IR powers.

### Rehydration Characteristics and Modeling

Figure 4 illustrates the rehydration behavior of the IR dried wormwood leaves where the variations in moisture content ( $\text{g}_{\text{water}} \text{g}^{-1} \text{ dry matter}$ ) of the leaves along the rehydration process at water temperature of  $80^\circ\text{C}$  are presented. From the figure, all curves show the same trends, where water uptake of the leaves increased significantly during the initial period of rehydration (accelerating absorption period) and then absorption rate slowed gradually (slow absorption period) until equilibrium moisture. Filling of capillaries and cavities near the surface of the leaves is the main reason for the quick initial water absorption. As water absorption proceeds, free capillaries and intercellular spaces are filled with water, leading to a decline in the soaking rate. The same observations have been reported by other researchers for hot air-dried quinces (Noshad *et al.*, 2012), fluid-bed and halogen dried carrots (Planinic' *et al.*, 2005), microwave-dried amaranth leaves (Mujaffar and Loy, 2016) and hot-air dried figs (Ansari *et al.*, 2015). Furthermore, based on the obtained results, rehydration capacity of leaves increased with increasing IR drying powers. The equilibrium moisture content values for the leaves dried at 200, 300, 400, and 500W was

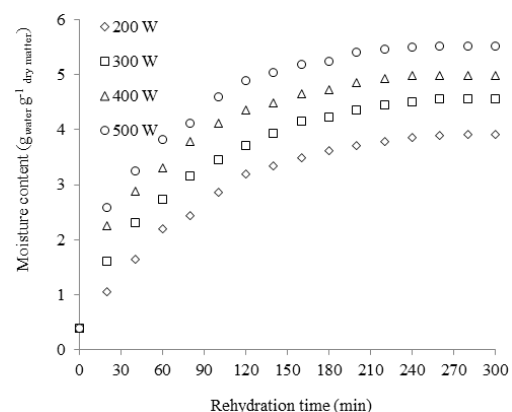


**Figure 4.** Variations in moisture content ( $\text{g}_{\text{water}} \text{g}^{-1} \text{ dry matter}$ ) of the wormwood leaves dried at different IR power levels with rehydration time.

obtained to be 3.91, 4.55, 4.98 and 5.51  $\text{g}_{\text{water}} \text{g}^{-1}_{\text{dry matter}}$ , respectively, during rehydration process. In fact, higher infrared powers lead to warmer drying chamber and may cause more porous structures which lead to higher water penetration. This observation is in agreement with the results reported in the literature by Noshad *et al.* (2012) for quinces, and Mujaffar and Loy (2016) for amaranth leaves.

The Peleg model was used to model moisture absorption kinetics of the leaves and the obtained values for Peleg rate constant ( $k_1$ ) and capacity constant ( $k_2$ ) for the applied drying temperatures with the statistical results ( $R^2$ ) are shown in Table 2. The Peleg rate constant is generally considered to be related to the mass transfer rate as the lower  $k_1$  value indicates the higher initial absorption rate. The capacity constant is inversely related to the absorption ability of foods. In all IR powers, the coefficients of determination were found to be high ( $R^2 > 0.99$ ) representing a good fit of the experimental data to the Peleg model. The kinetic rate constant and capacity constant were obtained to be in the range of 12.82-27.78 minutes  $(\text{g}_{\text{water}} \text{g}^{-1}_{\text{dry matter}})^{-1}$  and 0.1957-0.2849  $(\text{g}_{\text{water}} \text{g}^{-1}_{\text{dry matter}})^{-1}$ , respectively. Both of the constants changed inverse proportionally with the infrared power. Decreasing of the Peleg model parameters with drying temperature has been reported by some researchers such as Dadali *et al.* (2008), Demirhan and Özbek (2010), and Mujaffar and Loy (2016). Furthermore, the obtained values for the Peleg model in this study are comparable with the values reported in the literature for different

products (Dadali *et al.*, 2008; Demirhan and Özbek, 2010; Planinic *et al.*, 2005).

### Effect of Drying Process on Essential Oil Yield

Essential oil extracted from the wormwood leaves was dark green. The average essential oil yields extracted from the fresh and leaves dried at IR powers of 200, 300, 400, and 500W were obtained to be 1.718, 2.229, 1.908, 1.634, and 1.556  $\text{g}_{100} \text{g}^{-1}_{\text{dry matter}}$ , respectively. Infrared drying affected the essential oil value where the dehydration process of the leaves before distillation led to both increment and decrement in essential oil yield. Some researchers have found the same observation for different medicinal plants such as *Laurus nobilis* L. leaves (Sellami *et al.*, 2011), peppermint leaves (Torki-Harchegani *et al.*, 2016a) and thyme plants (Rahimmalek and Goli, 2013). Generally, temperature and duration of drying are the two main factors influencing the essential oil yield of plant materials as, depending on the factors, drying process can increase and/or decrease amount of essential oil content (Torki-Harchegani *et al.*, 2016a). The maximum and the minimum essential oil values were obtained from the leaves dried at infrared powers of 200 W (2.229  $\text{g}_{100} \text{g}^{-1}_{\text{dry matter}}$ ) and 500 W (1.556  $\text{g}_{100} \text{g}^{-1}_{\text{dry matter}}$ ), respectively. Furthermore, the obtained results indicate that any increment in applied infrared power level decreased significantly the essential oil yield. Similar observation was also found by Sellami *et al.* (2011).

**Table 2.** Values of the Peleg model parameters with statistical analysis for the wormwood leaves.

IR power (W)	$k_1$ [min $(\text{g}_{\text{water}} \text{g}^{-1}_{\text{dry matter}})^{-1}$ ]	$k_2$ $(\text{g}_{\text{water}} \text{g}^{-1}_{\text{dry matter}})^{-1}$	$R^2$
200	27.78	0.2849	0.9991
300	20.83	0.2410	0.9997
400	16.67	0.2183	0.9971
500	12.82	0.1957	0.9960



## Energy Consumption

The *SEC* value for infrared drying of the leaves at power levels of 200, 300, 400, and 500W was obtained to be 5.42, 6.39, 6.97 and 5.81 MJ kg<sup>-1</sup>, respectively. The obtained *SEC* values are comparable with those reported in the literature for different products. Toriki-Harchegani *et al.* (2016a) dried peppermint leaves using a microwave oven at power levels of 200, 400, 600, and 800W and determined the *SEC* values to be 4.58, 5.56, 5.89 and 5.24 MJ kg<sup>-1</sup>, respectively, respectively. Barzegar *et al.* (2015) investigated energy consumption during hot air-assisted drying of green pea at different conditions and found specific energy consumption values varied from 0.23 to 34.69 MJ kg<sup>-1</sup>. Darvishi (2012) studied microwave drying of apple slices at power densities of 5, 10, 15, and 20W g<sup>-1</sup> and obtained *SEC* values in the range of 4.22–10.56 MJ kg<sup>-1</sup>.

## CONCLUSIONS

The effect of infrared power output on drying and rehydration characteristics and also energy consumption and essential oil yield of wormwood leaves were studied. IR power had significant effect on drying time where the average process duration at IR powers of 200, 300, 400, and 500 W were 56, 44, 36, and 24 minutes, respectively. Drying rate increased rapidly during a short initial period and followed by a falling period. Among the applied thin layer models, the diffusion approach model showed the best fitting accuracy. Effective moisture diffusivity for the leaves varied from  $8.84 \times 10^{-8}$  to  $2.76 \times 10^{-7}$  m<sup>2</sup> s<sup>-1</sup> as infrared power increased from 200 to 500W.

The equilibrium moisture of the rehydrated leaves was increased with increasing IR power. The Peleg model described the experimental rehydration curves with high coefficient of determination. Drying of the leaves resulted in both increment and decrement in essential

oil yield where the extracted essential oil from the fresh leaves was 1.718 g 100 g<sup>-1</sup> dry matter. Increasing infrared power level decreased the essential oil yield. Specific energy consumption ranged from 4.22 to 10.56 MJ kg<sup>-1</sup>, corresponding to the maximum and the minimum values obtained for infrared power levels of 200 and 400W, respectively.

## REFERENCES

1. Akhondi, E., Kazemi, A. and Maghsoodi, V. 2011. Determination of a Suitable Thin Layer Drying Curve Model for Saffron (*Crocus sativus* L) Stigmas in an Infrared Dryer. *Scientia Iranica C.*, **18**: 1397–1401.
2. Ansari, S., Maftoon-Azad, N., Hosseini, E., Farahnaky, A. and Asadi, G. 2015. Modeling Rehydration Behavior of Dried Figs. *J. Agr. Sci. Tech.*, **17**: 133–144.
3. Barzegar, M., Zare, D. and Stroshine, R. L. 2015. An Integrated Energy and Quality Approach to Optimization of Green Peas Drying in a Hot Air Infrared-Assisted Vibratory Bed Dryer. *J. Food Eng.*, **166**: 302–315.
4. Beigi, M. 2016. Energy Efficiency and Moisture Diffusivity of Apple Slices during Convective Drying. *Food Sci. Technol.*, **36**: 145–150.
5. Celma, A.R., Cuadros, F. and López-Rodríguez, F. 2009. Characterization of Industrial Tomato By-Products from Infrared Drying Process. *Food Bioprod. Process.*, **87**: 282–291.
6. Crank, J. 1975. *The Mathematics of Diffusion*. Second edition. Clarendon Press, Oxford.
7. Dadali, G., Demirhan, E. and Özbek, B. 2008. Effect of Drying Condition on Rehydration Kinetics of Microwave Dried Spinach. *Food Bioprod. Process.*, **86**: 235–241.
8. Darvishi, H. 2012. Energy Consumption and Mathematical Modeling of Microwave Drying of Potato Slices. *Agric. Eng. Int.: CIGR J.*, **14**: 94–102.
9. Demirhan, E. and Özbek, B. 2010. Rehydration Kinetics of Microwave-Dried Basil. *J. Food Process. Preserv.*, **34**: 664–680.

10. Doymaz, I. 2012 Drying of Pomegranate Seeds Using Infrared Radiation. *Food Sci. Biotechnol.*, **21**: 1269–1275.
11. Doymaz, I. 2014. Infrared Drying of Button Mushroom Slices. *Food Sci. Biotechnol.*, **23**: 723–729.
12. Doymaz, I. 2015. Infrared Drying Kinetics and Quality Characteristics of Carrot Slices. *J. Food Process. Preserv.*, **39**: 2738–2745.
13. Minaei, S., Motevali, A., Ahmadi, E. and Azizi, M. H. 2012. Mathematical Models of Drying Pomegranate Arils in Vacuum and Microwave Dryers. *J. Agr. Sci. Tech.*, **14**: 311–325.
14. Mujaffar, S. and Loy, A. L. 2016. The Rehydration Behavior of Microwave-Dried Amaranth (*Amaranthus dubius*) Leaves. *Food Sci. Nutr.*, doi: 10.1002/fsn3.406.
15. Noshad, M., Mohebbi, M., Shahidi, F. and Mortazavi, S. A. 2012. Kinetic Modeling of Rehydration in Air-Dried Quinces Pretreated with Osmotic Dehydration and Ultrasonic. *J. Food Process. Preserv.*, **36**: 383–392.
16. Onwude, D. I., Hashin, N., Janius, R. B., Nawi, N. M. and Abdan, K. 2016. Modeling the Thin-Layer Drying of Fruits and Vegetables: A Review. *Comprehensive Rev. Food Sci. Food Safety*, **15**: 559–618.
17. Planinic, M., Velic, D., Tomas, S., Bilic, M. and Bucic, A. 2005 Modelling of Drying and Rehydration of Carrots Using Peleg's Model. *Eur. Food Res. Technol.*, **221**: 446–451.
18. Puente-Díaz, L., Ah-Hen, K., Vega-Gálvez, A., Lemus-Mondaca, R. and Di Scala, K. 2013. Combined Infrared-Convective Drying of Mutra (*Ugni molinae Turcz*) Berries: Kinetic Modeling and Quality Assessment. *Dry. Technol.*, **31**: 329–338.
19. Rahimmalek, M. and Goli, S. A. H. 2013. Evaluation of Six Drying Treatments with Respect to Essential Oil Yield, Composition and Color Characteristics of *Thymy sdaenensis* subsp. *daenensis*. Celak Leaves. *Indust. Crop. Produ.*, **42**: 613–619.
20. Sacilik, K., Keskin, R. and Elicin, A. K. 2006. Mathematical Modeling of Solar Tunnel Drying of Thin Layer Organic Tomato. *J. Food Eng.*, **73**: 231–238.
21. Sharma, G. P., Verma, R. C. and Pathare, P. 2005. Mathematical Modeling of Infrared Radiation Thin Layer Drying of Onion Slices. *J. Food Eng.*, **71**: 282–286.
22. Sellami, I. H., Wannes, W. A., Bettaieb, I., Berrima, S., Chahed, T., Marzouk, B. and Limam, F. 2011. Qualitative and Quantitative Changes in the Essential Oil of *Laurus nobilis* L. Leaves as Affected by Different Drying Methods. *Food Chem.*, **26**: 691–769.
23. Šumic, Z., Vakula, A., Tepic, A., Cakarevic, J., Vitas, J. and Pavlic, B. 2016. Modeling and Optimization of Red Currants Vacuum Drying Process by Response Surface Methodology (RSM). *Food Chem.*, **203**: 465–475.
24. Torki-Harchegani, M., Ghanbarian, D., Ghasemi Pirbalouti, A. and Sadeghi, M. 2016a. Dehydration Behaviour, Mathematical Modeling, Energy Efficiency and Essential Oil Yield of Peppermint Leaves Undergoing Microwave and Hot Air Treatments. *Renew. Sust. Ener. Rev.*, **58**: 407–418.
25. Torki-Harchegani, M., Ghasemi-Varnamkhasti, M., Ghanbarian, D., Sadeghi, M. and Tohidi, M. 2016b. Dehydration Characteristics and Mathematical Modeling of Lemon Slices Undergoing Oven Treatment. *Heat Mass Trans.*, **52**: 281–289.
26. Torki Harchegani, M., Sadegi, M., Moheb, A., Tohidi, M. and Naghavi, Z. 2012. Experimental Study of Deep-Bed Drying Kinetics of Rough Rice. *Agric. Eng. Int.: CIGR J.*, **14**: 195–202.
27. Zomorodian, A. and Moradi, M. 2010. Mathematical Modeling of Forced Convection Thin Layer Solar Drying for *Cuminum cyminum*. *J. Agr. Sci. Tech.*, **12**: 401–408.



## تأثیر توان خشک کردن فرسوخ بر ویژگی‌های خشک شدن، مصرف انرژی و ویژگی‌های کیفی برگ‌های افسنتین (*Artemisia absinthium* L.)

م. بیگی

چکیده

در پژوهش حاضر، تأثیر توان خشک کردن فرسوخ بر ویژگی‌های خشک شدن، مصرف انرژی و مقدار اسانس برگ‌های افسنتین مطالعه شد. لایه‌های نازک از برگ‌ها در توان‌های 200، 300، 400 و 500 وات خشکانده شدند. مقادیر ضریب انتشار موثر رطوبت برگ‌ها در شرایط خشک کردن اعمال شده در محدوده  $8/84 \times 10^{-8}$  تا  $2/76 \times 10^{-7}$  متر مربع بر ثانیه به دست آمد. نمودارهای بازجذب آب برای برگ‌های خشک شده در دمای ثابت 80 درجه سلسیوس به دست آمدند و بر مدل پلگک برازش شدند. ظرفیت بازجذب آب برگ‌ها با افزایش توان خشک کردن فرسوخ کاهش یافت. در مقایسه با برگ‌های تازه، خشک کردن فرسوخ هم منجر به کاهش و هم باعث افزایش مقدار اسانس شد. بیشترین و کمترین مقدار اسانس به ترتیب از برگ‌های خشکانده شده در توان‌های 200 وات و 500 وات به دست آمد. انرژی ویژه مصرفی از 4/22 مگاژول بر کیلوگرم تا 10/56 مگاژول بر کیلوگرم متغیر بود.